PHYSICAL REVIEW LETTERS

Doped Mott Insulator as the Origin of Heavy-Fermion Behavior in LiV_2O_4

R. Arita,[1] K. Held,[2] A. V. Lukoyanov,[3] and V. I. Anisimov[4]

[1]*RIKEN (The Institute of Physical and Chemical Research), Wako, Saitama 351-0198, Japan*
[2]*Max-Planck-Institut für Festkörperforschung, 70569 Stuttgart, Germany*
[3]*Ural State Technical University-UPI, 620002 Yekaterinburg, Russia*
[4]*Institute of Metal Physics, Russian Academy of Science-Ural Division, 620219 Yekaterinburg, Russia*
(Received 11 January 2007; published 17 April 2007)

We investigate the electronic structure of LiV_2O_4, for which heavy-fermion behavior has been observed in various experiments, by the combination of the local density approximation and dynamical mean field theory. To obtain results at zero temperature, we employ the projective quantum Monte Carlo method as an impurity solver. Our results show that the strongly correlated a_{1g} band is a lightly doped Mott insulator which, at low temperatures, shows a sharp (heavy) quasiparticle peak just above the Fermi level, which is consistent with recent photoemission experiments by Shimoyamada *et al.* [Phys. Rev. Lett. **96**, 026403 (2006)].

The discovery of heavy-fermion (HF) behavior in the $3d$ material LiV_2O_4 [1] was a big surprise since this phenomenon was previously a hallmark of certain f electron compounds. But below a characteristic temperature $T_K \sim 28$ K, the linear specific heat coefficient (γ) [1], the magnetic susceptibility [1], the Grüneisen parameter [2], and the quadratic resistivity coefficient [3] are also for LiV_2O_4 extraordinarily large, similar to f electron HF compounds and much larger than in other transition metal oxides. From $\gamma \sim 420$ mJ/mol K^2, an effective mass enhancement of $m^*/m \sim 25$ was inferred [4]. Neutron scattering [5], nuclear magnetic resonance [6], and electron spin resonance [7], as well as muon spin relaxation experiments [8] indicate the existence of local magnetic moments, which is consistent with a Curie-Weiss susceptibility [1] in the temperature range 50 to 1000 K. Down to the lowest temperatures measured LiV_2O_4 remains a cubic spinel and no long-range magnetic, spin glass, or superconducting order was observed. More recently, also a sharp Kondoesque peak of width 10 meV was observed in photoemission experiments [9] just 4 meV above the Fermi energy E_F, with a strong temperature dependence similar to that of other HF compounds. This finding is supported by the measurement of the magnetic curves at $T = 1.3$ K [10], which also suggests the existence of a sharp peak slightly above E_F.

The explanation of the HF behavior in LiV_2O_4 has been a challenge since its discovery. Local density approximation (LDA) calculations [4,11,12] show a twofold-degenerate and 2 eV wide e_g^π and a nondegenerate a_{1g} band of width 1 eV cross the Fermi energy, filled altogether with 1.5 electrons per V ion. This LDA band structure led one of the present authors (V. I. A.) to the proposal [11,13] that the a_{1g} electrons play the role of the localized f electrons in conventional HF compounds and the e_g^π electrons that of the itinerant valence electrons. On the other hand, the importance of geometrical frustration originating

in the spinel structure has been stressed by various authors [14–22], all suggesting different explanations for the mass enhancement of LiV_2O_4. Naturally the geometrical frustration suppresses any kind of long-range order, so that local spin or orbital fluctuations should be dominant as suggested in Refs. [20,21].

In this situation, we might expect dynamical mean field theory (DMFT) [23] to be a good approximation for studying the electronic correlations in this material. Realistic LDA + DMFT [24] calculations for LiV_2O_4 have been carried out before [25], but neglected the a_{1g}-e_g^π hybridization, which should be the driving force for the HF behavior in the Kondo scenario [11] and were furthermore restricted to temperatures $T > 750$ K, far above T_K. Not surprisingly, a quasiparticle resonance was not found and the competition between antiferromagnetic direct exchange from the a_{1g}-a_{1g} hybridization, ferromagnetic double exchange from the e_g^π-e_g^π hybridization, and the Kondo effect from the (neglected) a_{1g}-e_g^π hybridization left this LDA + DMFT study [25] inconclusive. Since that time the more sophisticated projection onto Wannier functions has been developed [26] which properly takes the orbital off-diagonal hybridization into account. Also, the problem that conventional quantum Monte Carlo (QMC) simulations [27] of the DMFT impurity problem were restricted to rather high temperatures because the numerical effort is proportional to $1/T^3$ has been overcome by the projective QMC (PQMC) method [28–30] for $T = 0$.

With these improvements, we reinvestigate LiV_2O_4 by LDA + DMFT(PQMC) and solve the puzzle of why this material shows HF behavior with a sharp Kondoesque resonance above the Fermi level.

Method.—The unit cell of LiV_2O_4 contains four V atoms and each V atom has three t_{2g} orbitals, which are split into the a_{1g} orbital and two degenerate e_g^π orbitals due to the trigonal splitting. First, we do a LDA calculation for LiV_2O_4 using the linearized muffin tin orbital basis set

[31]. From this we further construct an effective 12×12 Hamiltonian by the projection onto Wannier functions [26]. Since the e_g^π orbitals are degenerate, it is possible to derive a 2-orbital model with an 8×8 Hamiltonian by taking only one of two e_g^π orbitals into account. This drastically decreases the computational efforts of the LDA + DMFT calculation and hence allows for more accurate data. As we will see *a posteriori*, the restriction to one e_g^π orbital will be justified by the fact that the e_g^π orbitals play a rather passive role and the physics is determined by the a_{1g} band. The comparison of the band dispersion of this simplified 8-band model with total LDA band structure of LiV$_2$O$_4$ in Fig. 1 shows that the 2-orbital simplification captures the essential features of the real compound's band structure. It also gives the densities of states (DOS) close to that previously reported by LDA, see Fig. 5 in [25].

Second, we supplement this 2-orbital Hamiltonian by local intraorbital (U) and interorbital (U') Coulomb repulsions as well as by Hund's exchange (J), and solve the constructed many-body model by DMFT. It should be noted that we explicitly consider the off-diagonal elements between e_g^π and a_{1g} in contrast to all previous calculations [25], where only the initial LDA a_{1g}-e_g^π hybridization is reflected indirectly in the DOS. This a_{1g}-e_g^π hybridization is essential for the Kondo effect with localized a_{1g} and itinerant e_g^π electrons [11]. As for the self-energy, we only consider the diagonal element, so that the effective DMFT impurity model becomes a two-orbital problem. We also assume that the Hund coupling is of Ising type since simulating the SU(2) symmetric Hund coupling is difficult in QMC. The application of new, more sophisticated algorithms to this end, such as [32], remains an important challenge for the future.

Besides conventional QMC, we employed the PQMC method in the present LDA + DMFT calculation, basically following Refs. [28–30] for calculating ground state expectation values. With an imaginary time discretization $\Delta\tau = 0.267$ eV^{-1}, we take $\mathcal{L} = 20$ time slices for measurement and $\mathcal{P} = 65$ time slices before and thereafter for

projection. For the remaining imaginary time to $\tilde{\beta} = \infty$, we use the noninteracting Hamiltonian with a shifted one-particle potential so that we have $n = 1$ electrons per site for the a_{1g} orbitals and $n = 0.25$ for the e_g^π orbitals. This shift warranties (approximately) the same large-τ asymptotic behavior as the interacting Hamiltonian. We performed $\sim 3 \times 10^8$ QMC sweeps and used the maximum entropy method for calculating the spectral function $A(\omega)$ and the Fourier transformation of the Green function from imaginary time to frequencies, i.e., from $G(\tau)$ to $G(i\omega)$.

Results.—Let us start with the results of conventional QMC at finite T. In Fig. 2, we plot the spectral function $A(\omega)$, using Coulomb interaction parameters which are typical for $3d$ orbitals, i.e., $U = 3.6$, $U' = 2.4$, and $J = 0.6$ eV. The qualitative feature of the result for $\beta \equiv 1/T = 10$ eV^{-1} corresponding to $T \approx 1200$ K is similar to that of the previous LDA + DMFT calculation [25]. But for $\beta = 40$ eV^{-1} ($T \approx 300$ K) we note the emergence of a small structure in the a_{1g} band just above E_F, which is absent for $T \approx 1200$ K. At the same time, we see no noteworthy temperature dependence for the e_g^π band, especially around E_F (see the inset of Fig. 2). As far as the finite-T QMC is concerned, it is not clear whether the small structure in the a_{1g} band becomes a sharp quasiparticle peak at lower temperatures.

To clarify this point, let us now turn to the PQMC results at $T = 0$; see Fig. 3. Indeed we can see in the PQMC spectrum that the small structure just above E_F at $T \approx 300$ K becomes a sharp peak, which is consistent with the experiment [9], i.e., a peak 4 meV above E_F whose width is
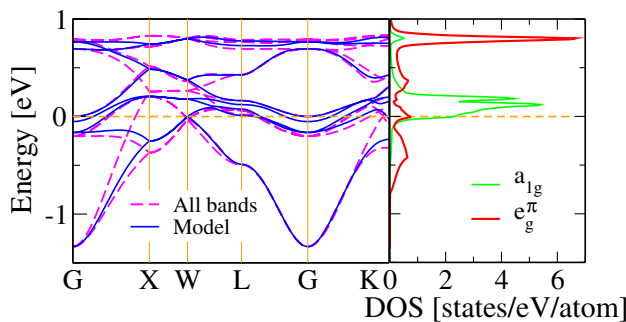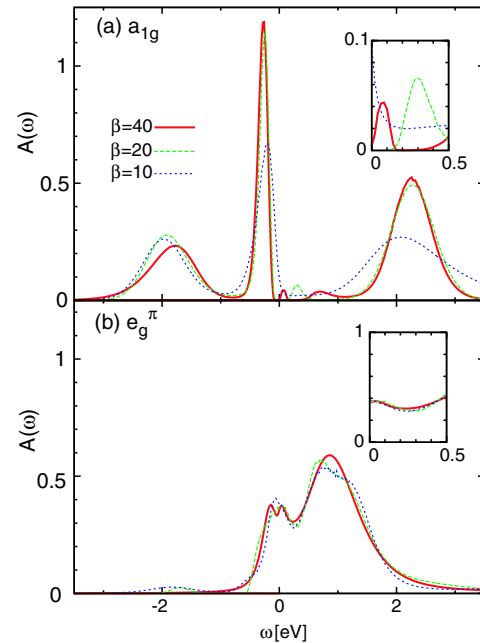

FIG. 1 (color online). Left panel: Band dispersion of the effective 2-orbital model (solid line) and total band structure (dashed line) of LiV$_2$O$_4$. Right panel: partial a_{1g} and e_g^π DOS for the model. E_F is set to zero.

FIG. 2 (color online). Spectral function of LiV$_2$O$_4$ at $\beta = 10$, 20, and 40 eV^{-1} ($T \approx 1200$, 600, and 300 K); $U = 3.6$, $U' = 2.4$, and $J = 0.6$ (all units are in eV). The insets show a close-up view immediately above E_F ($\omega = 0$).
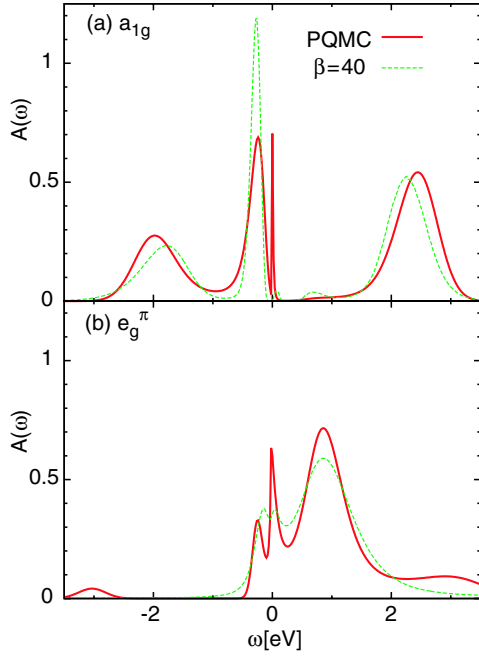
FIG. 3 (color online). Same as Fig. 2 but now at $T = 0$ (PQMC), compared to $\beta = 40$ eV^{-1} corresponding to $T \approx$ 300 K. In agreement with experiment, we can see a sharp peak slightly above E_F (set to zero) in the a_{1g} band.

FIG. 4 (color online). Green function for the a_{1g} (a) and e_g^π (b) orbitals obtained by LDA + DMFT(PQMC) as a function of τ, compared with the result for $\beta = 40$ eV^{-1} ($T \approx$ 300 K). In the inset, we magnify the region $\tau > 1$.

10 meV. This a_{1g} band is lightly doped, containing $n = 0.98$ electrons per site. Unfortunately, the exact determination of the renormalization factor (Z) from $A(\omega)$ or the self-energy is difficult because of the smallness of the structure and fluctuations from iteration to iteration in the DMFT cycle. However, the peak itself is stable as is the behavior of $G(\tau)$, plotted in Fig. 4. The latter shows a very slow decay for large τ in PQMC which necessitates the existence of a sharp peak at small positive energies in the a_{1g} band. In contrast, for $T \approx$ 300 K, $G(\tau)$ vanishes exponentially; see Fig. 4(a).

Discussion.—Let us now turn to the physical origin of the sharp peak in the a_{1g} band. One possible scenario which was originally proposed in Ref. [11] is the Kondo effect caused by the hybridization between a_{1g} and e_g^π orbitals on neighboring sites (note that the on site hybridization is absent). However, it is not trivial whether the associated (antiferromagnetic) Kondo coupling is strong enough to survive a Hund's exchange coupling as large as $J = 0.6$.

To single out the effect of the a_{1g}-e_g^π hybridization, we perform an auxiliary LDA + DMFT calculation. To this end, we first obtain the a_{1g} and e_g^π LDA DOS from the effective 2-orbital Hamiltonian and then do DMFT calculations with these DOSes without any hybridization. We plot the resulting $G(\tau)$ and $A(\omega)$ of the a_{1g} band in Fig. 5. Clearly, the sharp peak just above E_F survives switching off the a_{1g}-e_g^π hybridization. Hence, we can conclude that the Kondo scenario due to the hybridization with e_g^π orbitals [11] cannot be the microscopic origin for the peak in
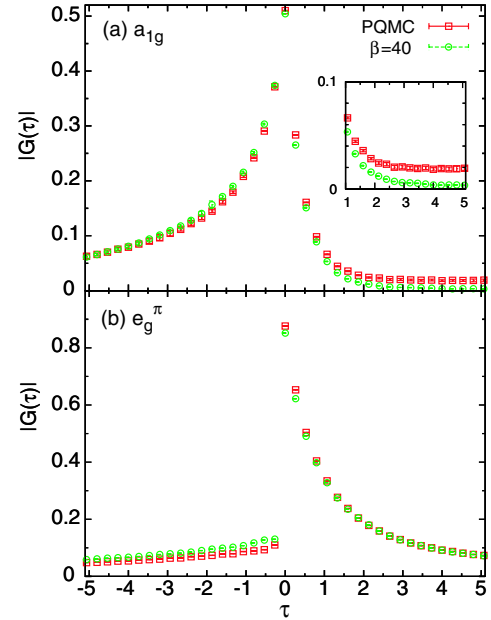
the a_{1g} band. Actually, besides contributing to the doping of the a_{1g} band, the e_g^π electrons do not play a pronounced role and are only weakly correlated. Their self-energy (not shown) is almost constant down to very low frequencies ~ 0.01 eV. The constant (Im$\Sigma \sim -0.14$ eV) can be explained by noninteracting electrons scattering at disordered spins, which is an appropriate description of the a_{1g} electrons except for the lowest energies.

Hence, let us turn to the a_{1g} band itself which is not exactly half-filled, but lightly doped with $n \sim 0.98$ electrons per site. This suggests that the a_{1g} band is a lightly hole-doped Mott insulator with a very strongly renormalized quasiparticle because of the nearness to the doping-controlled Mott-Hubbard transition. We can compare our results with those of Ref. [33] for the single-band Hubbard model on the hypercubic lattice. At $n = 0.97$ and very low temperature, these results show a sharp peak just above E_F [33], very similar to our LDA + DMFT calculations. An important question for this scenario of a doped Mott insulator is whether the strong renormalizations can survive the presence of short-range correlations beyond DMFT. In this respect, the correlator projection method indicates that Z does not vanish for the filling-control Mott-Hubbard transition in the two-dimensional Hubbard model [34], and also the dynamical vertex approximations [35] show a strong damping of the quasiparticle peak in the vicinity of the Mott-Hubbard transition due to antiferromagnetic fluctuations beyond DMFT. However, we believe that such effects are less relevant for LiV$_2$O$_4$ because of the frustrated three-dimensional lattice and because there is no
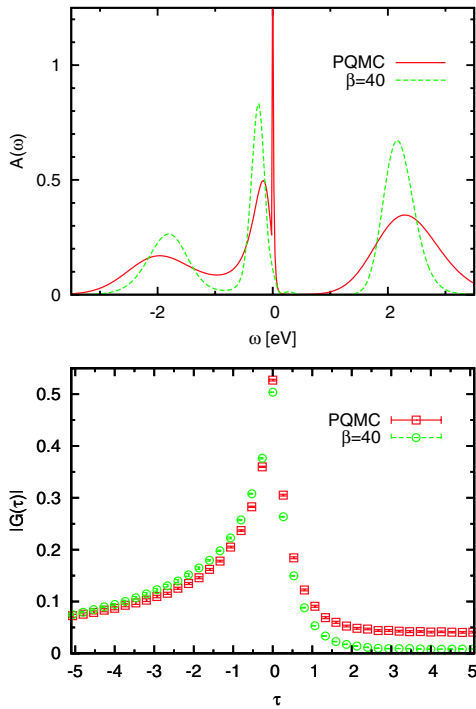
FIG. 5 (color online). Spectrum (top) and Green function (bottom) of the a_{1g} band without a_{1g}-e_g^π hybridization. The sharp peak above E_F survives if the hybridization is switched off.

indication that the system is close to a magnetic phase transition.

In conclusion, realistic LDA + DMFT calculations for LiV$_2$O$_4$ show a sharp peak for $T \to 0$ in agreement with photoemission experiments and large renormalizations of the effective mass. The physical origin of this peak is the lightly doping of the a_{1g} band which is hence metallic but very close to a Mott-Hubbard transition. The HF physics is not caused by the hybridization between localized a_{1g} and itinerant e_g^π orbitals. Instead, the a_{1g} orbitals play both roles simultaneously, whereas the e_g^π orbitals are rather passive and not strongly correlated.

[1] S. Kondo *et al.*, Phys. Rev. Lett. **78**, 3729 (1997).
[2] O. Chmaissem *et al.*, Phys. Rev. Lett. **79**, 4866 (1997).
[3] C. Urano *et al.*, Phys. Rev. Lett. **85**, 1052 (2000).
[4] J. Matsuno, A. Fujimori, and L. F. Mattheiss, Phys. Rev. B **60**, 1607 (1999).
[5] A. Krimmel *et al.*, Phys. Rev. Lett. **82**, 2919 (1999); Phys. Rev. B **61**, 12578 (2000); S.-H. Lee *et al.*, Phys. Rev. Lett. **86**, 5554 (2001).
[6] N. Fujiwara, H. Yasuoka, and Y. Ueda, Phys. Rev. B **57**, 3539 (1998); A. V. Mahajan *et al.*, Phys. Rev. B **57**, 8890 (1998).
[7] M. Lohmann *et al.*, Physica (Amsterdam) **259–261B**, 963 (1999).
[8] A. Koda *et al.*, Phys. Rev. B **69**, 012402 (2004).
[9] A. Shimoyamada *et al.*, Phys. Rev. Lett. **96**, 026403 (2006).
[10] S. Niitaka *et al.*, J. Magn. Magn. Mater. **310**, e258 (2007).
[11] V. I. Anisimov *et al.*, Phys. Rev. Lett. **83**, 364 (1999).
[12] V. Eyert *et al.*, Europhys. Lett. **46**, 762 (1999).
[13] Also note H. Kusunose, S. Yotsuhashi, and K. Miyake, Phys. Rev. B **62**, 4403 (2000).
[14] C. Lacroix, Can. J. Phys. **79**, 1469 (2001).
[15] N. Shannon, Eur. Phys. J. B **27**, 527 (2002).
[16] P. Fulde *et al.*, Europhys. Lett. **54**, 779 (2001).
[17] S. Burdin, D. R. Grempel, and A. Georges, Phys. Rev. B **66**, 045111 (2002).
[18] J. Hopkinson and P. Coleman, Phys. Rev. Lett. **89**, 267201 (2002).
[19] S. Fujimoto, Phys. Rev. B **65**, 155108 (2002).
[20] H. Tsunetsugu, J. Phys. Soc. Jpn. **71**, 1844 (2002).
[21] Y. Yamashita and K. Ueda, Phys. Rev. B **67**, 195107 (2003).
[22] M. S. Laad, L. Craco, and E. Müller-Hartmann, Phys. Rev. B **67**, 033105 (2003).
[23] W. Metzner and D. Vollhardt, Phys. Rev. Lett. **62**, 324 (1989); A. Georges and G. Kotliar, Phys. Rev. B **45**, 6479 (1992); A. Georges *et al.*, Rev. Mod. Phys. **68**, 13 (1996).
[24] V. I. Anisimov *et al.*, J. Phys. Condens. Matter **9**, 7359 (1997); A. I. Lichtenstein and M. I. Katsnelson, Phys. Rev. B **57**, 6884 (1998); K. Held *et al.*, Phys. Status Solidi B **243**, 2599 (2006); cond-mat/0511293; G. Kotliar *et al.*, Rev. Mod. Phys. **78**, 865 (2006).
[25] I. A. Nekrasov *et al.*, Phys. Rev. B **67**, 085111 (2003).
[26] V. I. Anisimov *et al.*, Phys. Rev. B **71**, 125119 (2005).
[27] J. E. Hirsch and R. M. Fye, Phys. Rev. Lett. **56**, 2521 (1986).
[28] M. Feldbacher, K. Held, and F. F. Assaad, Phys. Rev. Lett. **93**, 136405 (2004).
[29] R. Arita and K. Held, Phys. Rev. B **72**, 201102 (2005).
[30] R. Arita and K. Held, Phys. Rev. B **73**, 064515 (2006).
[31] O. K. Andersen, Phys. Rev. B **12**, 3060 (1975); O. Gunnarsson, O. Jepsen, and O. K. Andersen, Phys. Rev. B **27**, 7144 (1983).
[32] S. Sakai *et al.*, Phys. Rev. B **74**, 155102 (2006).
[33] Th. Pruschke, D. L. Cox, and M. Jarrell, Phys. Rev. B **47**, 3553 (1993).
[34] K. Hanasaki and M. Imada, J. Phys. Soc. Jpn. **75**, 084702 (2006).
[35] A. Toschi, A. Katanin, and K. Held, Phys. Rev. B **75**, 045118 (2007).